

We are IntechOpen, the world's leading publisher of Open Access books Built by scientists, for scientists

6,900

Open access books available

186,000

International authors and editors

200M

Downloads

Our authors are among the

154

Countries delivered to

TOP 1%

most cited scientists

12.2%

Contributors from top 500 universities



WEB OF SCIENCE™

Selection of our books indexed in the Book Citation Index
in Web of Science™ Core Collection (BKCI)

Interested in publishing with us?
Contact book.department@intechopen.com

Numbers displayed above are based on latest data collected.
For more information visit www.intechopen.com



Radar Meteor Detection: Concept, Data Acquisition and Online Triggering

Eric V. C. Leite¹, Gustavo de O. e Alves¹, José M. de Seixas¹,
Fernando Marroquim², Cristina S. Vianna² and Helio Takai³

¹*Federal University of Rio de Janeiro/Signal Processing Laboratory/COPPE-Poli*

²*Federal University of Rio de Janeiro/Physics Institute*

³*Brookhaven National Laboratory*

^{1,2}*Brazil*

³*USA*

1. Introduction

In the solar system, debris whose mass ranges from a few micrograms to kilograms are called meteoroids. By penetrating into the atmosphere, a meteoroid gives rise to a meteor, which vaporizes by sputtering, causing a bright and ionized trail that is able to scatter forward Very High Frequency (VHF) electromagnetic waves. This fact inspired the Radio Meteor Scatter (RMS) technique (McKinley, 1961). This technique has many advantages over other meteor detection methods (see Section 2.1): it works also during the day, regardless of weather conditions, covers large areas at low cost, is able to detect small meteors (starting from micrograms) and can acquire data continuously. Not only meteors trails, but also many other atmospheric phenomena can scatter VHF waves and may be detected, such as lightning and e-clouds.

The principle of RMS detection consists in using analog TV stations, which are constantly switched on and broadcasting VHF radio waves, as transmitters of opportunity in order to build a passive bistatic radar system (Willis, 2008). The receiver station is positioned far away from the transmitter, sufficiently to be below the horizon line, so that signal cannot be directly detected as the ionosphere does not usually reflect electromagnetic waves in VHF range (30 - 300 MHz)(Damazio & Takai, 2004). The penetration of a meteor on Earth's atmosphere creates this ionized trail, which is able to produce the forward scattering of the radio waves and the scattered signals eventually reach the receiver station.

Due to continuous acquisition, a great amount of data is generated (about 7.5 GB, each day). In order to reduce the storage requirement, algorithms for online filtering are proposed in both time and frequency domains. In time-domain the matched filter is applied, which is optimal in the sense of the signal-to-noise ratio when the additive noise that corrupts the received signal is white. In frequency-domain, an analysis of the power spectrum is applied.

The chapter is organized as it follows. The next section presents the meteor characteristics, and briefly introduces the several detection techniques. Section 3 describes the meteor radar detection and the experimental setup. Section 4 shows the online triggering algorithm performance for real data. Finally, conclusions and perspectives are addressed in Section 5.

2. Meteors

Meteoroids are mostly debris in the Solar System. The visible path of a meteoroid that enters Earth's (or another body's) atmosphere is called a meteor (see Fig. ??). If a meteor reaches the ground and survives impact, then it is called a meteorite. Many meteors appearing seconds or minutes apart are called a meteor shower. The root word meteor comes from the Greek *μετεωρον*, meaning "high in the air". Very small meteoroids are known as micrometeoroids, 1g or less.

Many of meteoroid characteristics can be determined as they pass through Earth's atmosphere from their trajectories, position, mass loss, deceleration, the light spectra, etc of the resulting meteor. Their effects on radio signals also give information, especially useful for daytime meteor, cloudy days and full moon nights, which are otherwise very difficult to observe. From these trajectory measurements, meteoroids have been found to have many different orbits, some clustering in streams often associated with a parent comet, others apparently sporadic. Debris from meteoroid streams may eventually be scattered into other orbits. The light spectra, combined with trajectory and light curve measurements, have yielded various meteoroid compositions and densities. Some meteoroids are fragments from extraterrestrial bodies. These meteoroids are produced when these are hit by meteoroids and there is material ejected from these bodies.

Most meteoroids are bound to the Sun in a variety of orbits and at various velocities. The fastest ones move at about 42 km/s with respect to the Sun since this is the escape velocity for the solar system. The Earth travels at about 30 km/s with respect to the Sun. Thus, when meteoroids meet the Earth's atmosphere head-on, the combined speed may reach about 72 km/s.

A meteor is the visible streak of light that occurs when a meteoroid enters the Earth's atmosphere. Meteors typically occur in the mesosphere, and most range in altitude from 75 to

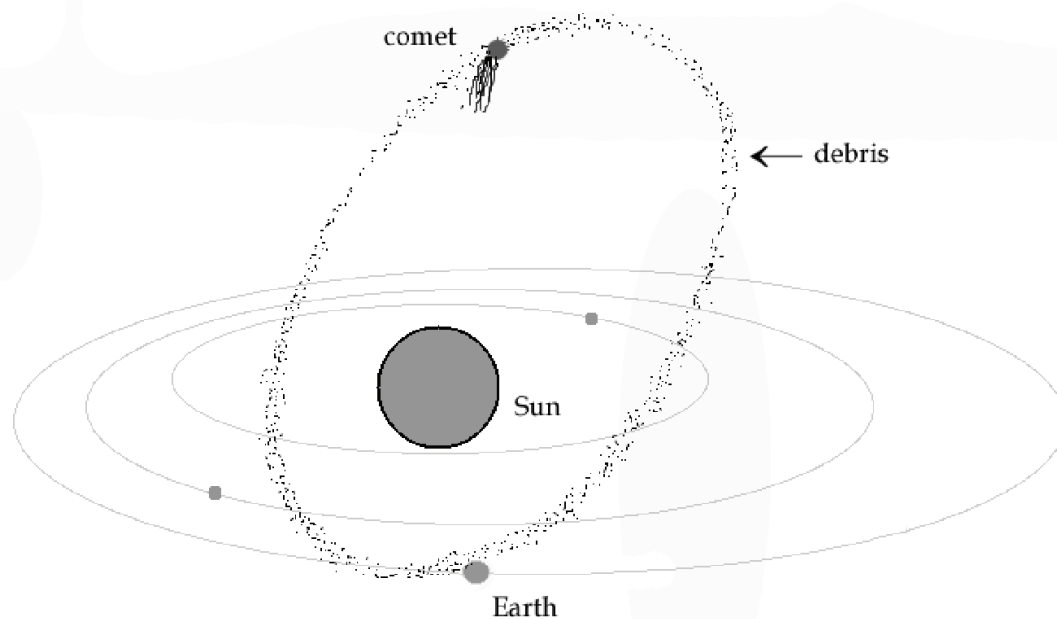


Fig. 1. Debris left by a comet may enter on Earth's atmosphere and give rise to a meteor.

100 km. Millions of meteors occur in the Earth's atmosphere every day. Most meteoroids that cause meteors are about the size of a pebble. They become visible in a range about 65 and 120 km above the Earth. They disintegrate at altitudes of 50 to 95 km. Most meteors are, however, observed at night as low light conditions allow fainter meteors to be observed.

During the entry of a meteoroid or asteroid into the upper atmosphere, an ionization trail is created, where the molecules in the upper atmosphere are ionized by the passage of the meteor (Int. Meteor Org., 2010). Such ionization trails can last up to 45 minutes at a time. Small, sand-grain sized meteoroids are entering the atmosphere constantly, essentially every few seconds in any given region of the atmosphere, and thus ionization trails can be found in the upper atmosphere more or less continuously.

Radio waves are bounced off these trails. Meteor radars can measure also atmospheric density, ozone density and winds at very high altitudes by measuring the decay rate and Doppler shift of a meteor trail. The great advantage of the meteor radar is that it takes data continuously, day and night, without weather restrictions. The visible light produced by a meteor may take on various hues, depending on the chemical composition of the meteoroid, and its speed through the atmosphere. This is possible to determine all important meteor parameters such as time, position, brightness, light spectra and velocity. Furthermore it is possible also to obtain light curves, meteor spectra and other special features. The radiant and velocity of a meteoroid yield its heliocentric orbit. This allows to associate meteoroid streams with parent comets. The deceleration gives information regarding the composition of the meteoroids. From statistical samples of meteor heights several distinct groups with different genetic origins have been deduced.

2.1 Meteor observation methods

There are many ways to observe meteors:

- **Visual Meteor Observation** - Monitoring meteor activity by the naked eye. Least accurate method but easy to carry out in special by amateur astronomers. Large numbers of observations allow statistically significant results. Visual observations are used to monitor major meteor showers, sporadic activity and minor showers down to a zenithal hourly rate (ZHR) of 2. The observer can count and estimate the meteor magnitude using a tape recorder for later to plot a frequency histogram. The visual method is very limited since the observer cannot work during the day or cloudy nights. Such an observation can be quite unreliable when the total meteor activity is high e.g. more than 50 meteors per hour. The naked eye is able to detect meteors down to approximately +7mag under excellent circumstances in the vicinity of the center of the field of view (absolute magnitude - mag - is the stellar magnitude any meteor would have if placed in the observer's zenith at a height of 100 km. A 5th magnitude meteor is on the limit of naked eye visibility. The higher the positive magnitude, the fainter the meteor, and the lower the positive or negative number, the brighter the meteor).

- **Photographic Observations** - The meteors are captured on a photographic film or plate (Hirose & Tomita, 1950). The accuracy of the derived meteor coordinates is very high. Normal-lens photography is restricted to meteors brighter than about +1mag. Multiple-station photography allows the determination of precise meteoroid orbits.

Photographic methods can hardly compete with video advanced techniques. The effort to be spent for the observation equipment is much lower than for video systems. For this reason photographic observations is widely used by amateur astronomers. On the other hand, the photograph methods allow to obtain very important meteor parameters: accurate

position, height, velocity, etc. The sensitivity of the films must be considered. There is now very sensitive digital cameras with high resolution for affordable prices, which produce a great impact to this technique. This method is restricted also to clear nights.

- **Video Observations** - This technique uses a video camera coupled with an image intensifier to record meteors (Guang-jie & Zhou-sheng, 2004). The positional accuracy is almost as high as that of photographic observations and the faintest meteor magnitudes are comparable to visual or telescopic observations depending on the used lens. Meteor shower activity as well as radiant positions can be determined. Multiple-station video observations allow the determination of meteoroid orbits.

Advanced video techniques permit detection of meteors up to +8mag. Video observation is the youngest and one of the most advanced observing techniques for meteor detection. Professional astronomers started to use video equipment at the beginning of the seventies of the last century. Currently the major disadvantage is the considerable price of a video system.

- **Telescopic Observations** - This comprises monitoring meteor activity by a telescope, preferably binoculars. This technique is used to determine radiant positions of major and minor showers, to study meteors much fainter than those seen in visual observations ones, which may reach +11mag. Although the narrower field, the measurements are more precise.
- **Radio Observations** - Two main methods are used, forward scatter observations and radar observations. The first method is easy to carry out, but delivers only data on the general meteor activity. The last is carried out by professional astronomers. Meteor radiants and meteoroid orbits can be determined. Radar meteors as well as telescopic ones may be as faint as +11mag.

Radio meteor scatter is an ideal technique for observing meteors continuously, day and night and even in cloudy days. Meteor trails can reflect radio waves from distant transmitters back to Earth, so that when a meteor appears one can sometimes receive small portions of broadcasts from radio stations up to 2,000 km away from the observing site.

The technique is strongly growing in popularity amongst meteor amateur astronomers. In the recent years, some groups started automating the radio observations by monitoring the signal from the radio receiver with a computer and even in cloudy days (see Fig. 2). Even for such high performance, the interpretation of the observations is difficult. A good understanding of the phenomenon is mandatory.

3. Meteor radio detection

Measurements performed by Lovell in 1947 using radar technology of the time showed that some returned signals were from meteor trails. This was the start of a technique known today as RMS, which was intensely developed in the 50's and 60's. Both experimental and theoretical work have been developed. Today, radio meteor scatter can be easily implemented having in hands an antenna, a good radio receiver and a personal computer.

There are two basic radar arrangements: backscattering and forward scattering. Back scattering is the traditional radar, where the transmitting station is near the receiving antenna. Forward scattering is used when the transmitter is located far from the receiver. Both arrangements are used in the detection of meteors. Back scatter radar tends to be pulsed and forward scatter continuous wave (CW). Forward scatter radar shows an increase in sensitivity

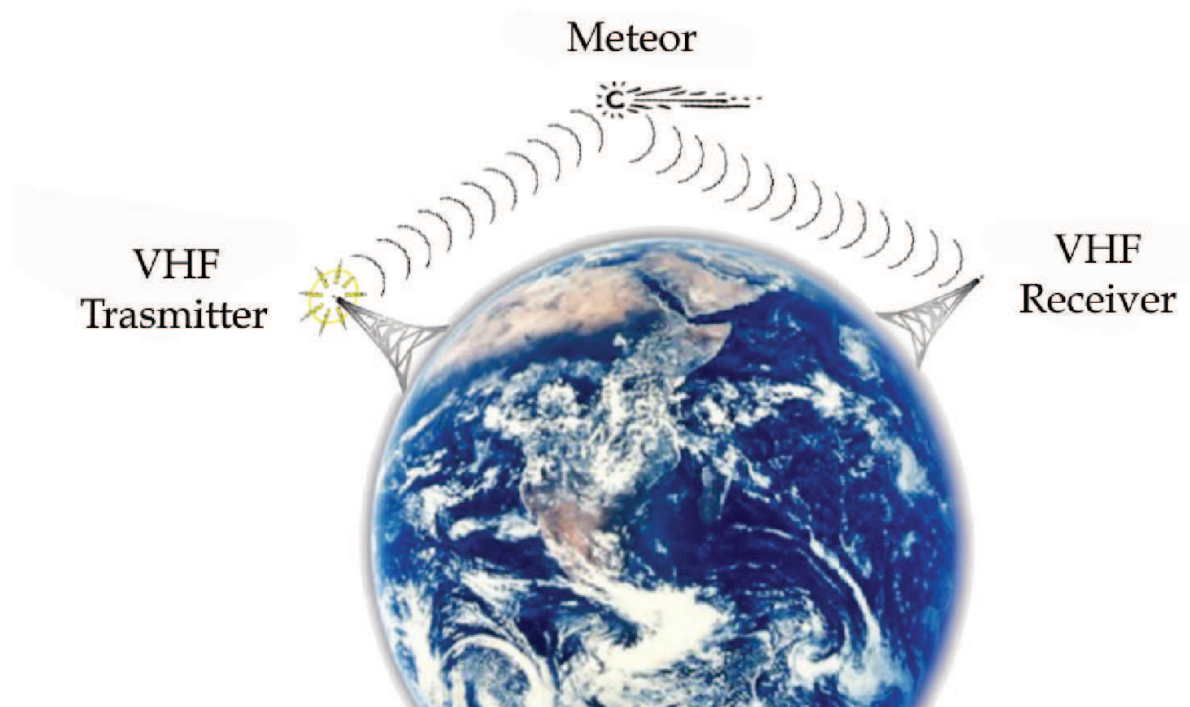


Fig. 2. RMS detection principle.

for the detection of small trails when compared to a same power backscatter due to the differences in aspect ratios. Forward scattering also avoids possible confusion of echos by the ionosphere as discussed by (Matano et al., 1968).

One of the main challenges to estimate the signal return power and its duration lies in a better understanding of the lower atmosphere chemical properties. At higher altitudes where meteors produce ionization trails, 80 to 120 km, the return signal duration only depends on the hot plasma diffusion rate. At lower altitudes, electron attachment to molecular oxygen limits the signal duration for their detection. In addition, the shorter mean free path causes the electron to scatter while radiating and therefore dampening the return power. An energy of $1eV$ electron will roughly undergo 10^9 collisions per second, or 10 collisions in a one wavelength at 100 MHz. The formalism to evaluate both signal duration and reflected power is well understood for meteor trails.

A specular reflection from an electron cloud only happens when a minimum free electron density is reached. This is known from plasma physics and is given by:

$$v_p = \sqrt{\frac{n_e e^2}{\pi m_e}} \quad (1)$$

where n_e , e and m_e are the electron density, charge and mass, respectively, which takes a value of $n_e = 3.8 \times 10^{13} m^{-3}$ for $f = 55.24 MHz$ (channel 2) and $n_e = 5.6 \times 10^{13} m^{-3}$ for $f = 67.26 MHz$ (channel 4). Below this critical density the reflection is partial and decreases with decreasing electron density. A total reflection happens because the electron density is high enough so that electrons reradiate energy from its neighbors. This happens in meteor trails that are usually called to be in an overdense scattering regime. The converse is the underdense, for which the density is lower and there is no re-radiation by electrons in the cloud. Both regimes are well

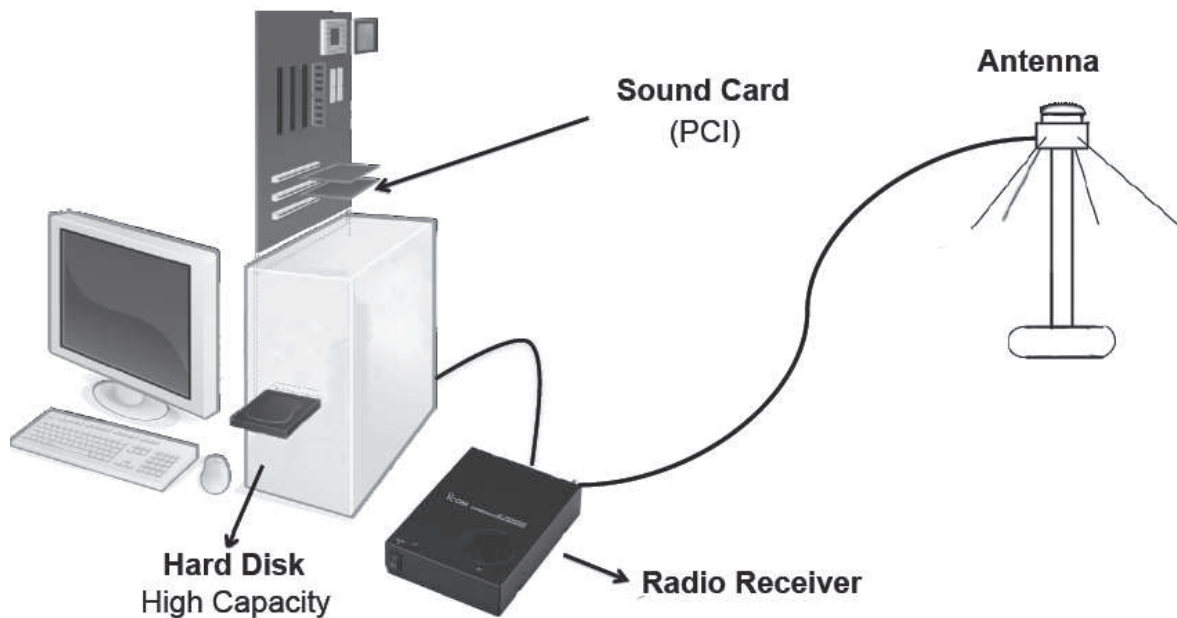


Fig. 3. Experimental setup for radar signal reception.

known from the radio meteor scatter science. Meteor ionization is produced at altitudes above 80 km where the atmosphere is rarefied and gases are from the meteor elements itself. The lifetime of the ionization trail produced by a meteor is a function of diffusion that cools the hot trail and recombination of electrons to the positive ions. Because of the elevated temperature the ionization lasts typically from 0.2 to 0.5 seconds.

The formalism to calculate the reflected power by a meteor trail is well developed both as a model and numerical integration. Models provide good means to understand the underlying processes and for the case of meteors they have been perfected over decades to provide reliable values for power at the receiver. Development of these models is driven by the application known as meteor burst communication where the ionization trails are used to bounce VHF for distances over 2,000 km.

3.1 Experimental setup

As an example, the setup for experimental data acquisition used here to quote the performance of the online detection algorithms is shown in Fig. 3. It includes a double dipole (in "V", inverted) antenna (Damazio & Takai, 2004) for a nearly vertical detection, a computer controlled radio receiver tuned to video carrier of an analog TV channel and a personal computer equipped with an off-board sound card, able to perform sampling rates up to 96 kHz. Due to continuous operation, a hard disk of high capacity is required.

4. Online triggering

The continuous acquisition is an inherent characteristic to radar technique. Acquiring data continuously means generating a great amount of data, which must be stored for a posterior analysis, or processed online for the extraction of the relevant information. Moreover, most of the data are from background noise events, which makes it difficult the detection of interesting events due to the data volume. If the online trigger is not implemented, the full data storage requires a more complex storage system, which increases the final cost of the experimental

setup. In other hand, if the data are processed online, only what is judged interesting will be retained, which translates into a significant reduction on the data volume to be stored.

In order to obtain an efficient detection and classification of received signals, online algorithms are designed in both time and frequency domains. In time-domain, the matched filter is applied. In frequency-domain, an analysis of the cumulative spectral power is applied. The next subsections provide a brief description of such techniques.

4.1 Signal detection

When the RMS (Radio Meteor Scatter) technique is considered, the signal detection problem can be formulated as the observation of a block of received data for decision among two hypotheses (Shamugan & Breipohl, 1998): H_0 , also called the null hypothesis, which states that only noise is present, and H_1 , also called the alternate hypothesis, which states that the block contains meteor signal masked by additive noise. In a simpler case, the signal to be detected may be known a priori (deterministic signal detection), and samples are corrupted by noise. Due to natural randomness of the occurrence of meteor events, the signal generated by them is considered as a stochastic process (Papoulis, 1965). Thus, from an observation Y of the incoming signal, $P(H_i|y)$ with $i = 0,1$ represents the probability, given a particular value $Y = y$, that H_i is true. The decision in favor of each hypothesis considers the largest probability: if $P(H_1|y) > P(H_0|y)$ choose H_1 , or if $P(H_0|y) > P(H_1|y)$ choose H_0 :

$$\frac{P(H_1|y)}{P(H_0|y)} \underset{H_0}{\overset{H_1}{\geq}} 1 \tag{2}$$

Through the Bayes' rule for conditional probabilities (Papoulis, 1965), we can write $P(H_i|y)$ as

$$P(H_i|y) = \frac{f_{Y|H_i}(y|H_i)P(H_i)}{f_Y(y)} \tag{3}$$

and the ratio in equation 2 becomes

$$\frac{f_{Y|H_1}(y|H_1)P(H_1)}{f_{Y|H_0}(y|H_0)P(H_0)} \underset{H_0}{\overset{H_1}{\geq}} 1 \tag{4}$$

or

$$\frac{f_{Y|H_1}(y|H_1)}{f_{Y|H_0}(y|H_0)} \underset{H_0}{\overset{H_1}{\geq}} \frac{P(H_0)}{P(H_1)} = \gamma. \tag{5}$$

The ratio at the left in Equation 5 is called the likelihood ratio, and the constant $P(H_0)/P(H_1) = \gamma$ is the decision threshold.

Due to noise interference and other practical issues, the detection system may commit mistakes. The meteor signal detection system performs a binary detection, so that two types of errors may occur:

- Type-I: Accept H_1 when H_0 is true (which means taking noise as a meteor signal and produce a false alarm).
- Type-II: Accept H_0 when H_1 is true (which means to miss a target signal).

The probability to commit a type-I error is called *false alarm probability*, denoted as P_F , and the probability of type-II error is called *probability of a miss* (P_M) (Shamugan & Breipohl, 1998). In addition, we can define $P_D = 1 - P_M$, which is called the detection probability. The decision threshold can be handled to produce acceptable values for both detection and false alarm probabilities. If the decision threshold is varied, the Receiver Operating Characteristics (ROC) curve can be constructed (Fawcett, 2006). This means to plot P_D versus P_F . As the signal-to-noise ratio (SNR) decreases, detection efficiency deteriorates, which translates into ROC curves near the diagonal and for a given fixed P_D , the false alarm probability increases. Therefore, the detection system can be designed by establishing the desired P_D and minimizing P_F , which is known as the Neyman-Parson detector (Trees - Part I, 2001). Another useful performance index is the sum-product (Anjos, 2006), which is defined as

$$SP = \frac{(P_D + 1 - P_F)}{2} (P_D(1 - P_F)). \quad (6)$$

By maximizing the SP index, a balanced detection efficiency is achieved for both hypotheses H_0 and H_1 .

4.2 The matched filter

In the case the signal to be detected is known (deterministic), from Equation 5, considering that the block of received data $s[n]$ comprises N samples and the additive noise is white (Trees - Part I, 2001), we have:

$$\frac{\prod_{i=1}^N f_{Y_i|H_1}(y_i|H_1)}{\prod_{i=1}^N f_{Y_i|H_0}(y_i|H_0)} \underset{H_0}{\overset{H_1}{\geq}} \gamma. \quad (7)$$

Now if the noise is Gaussian with zero mean and variance σ^2 , the Equation 7 becomes

$$\frac{\prod_{i=1}^N \frac{1}{\sqrt{(2\pi\sigma)}} \exp\left(-\frac{(y_i - s[i])^2}{2\sigma^2}\right)}{\prod_{i=1}^N \frac{1}{\sqrt{(2\pi\sigma)}} \exp\left(-\frac{y_i^2}{2\sigma^2}\right)} \underset{H_0}{\overset{H_1}{\geq}} \gamma. \quad (8)$$

Taking the natural logarithm and rearranging the terms, we have

$$\mathbf{y}^T \mathbf{s} \underset{H_0}{\overset{H_1}{\geq}} \sigma^2 \ln(\gamma) + \frac{1}{2} (\mathbf{s}^T \mathbf{s}) \quad (9)$$

or

$$\mathbf{y}^T \mathbf{s} \underset{H_0}{\overset{H_1}{\geq}} \gamma'. \quad (10)$$

Thus, in the presence of additive white Gaussian noise, the decision between the two hypotheses is given by the inner product between the received signal and a copy of the target signal. This approach is known as the matched filter, which is proved to be optimal in the sense of the signal-to-noise ratio (Trees - Part I, 2001).

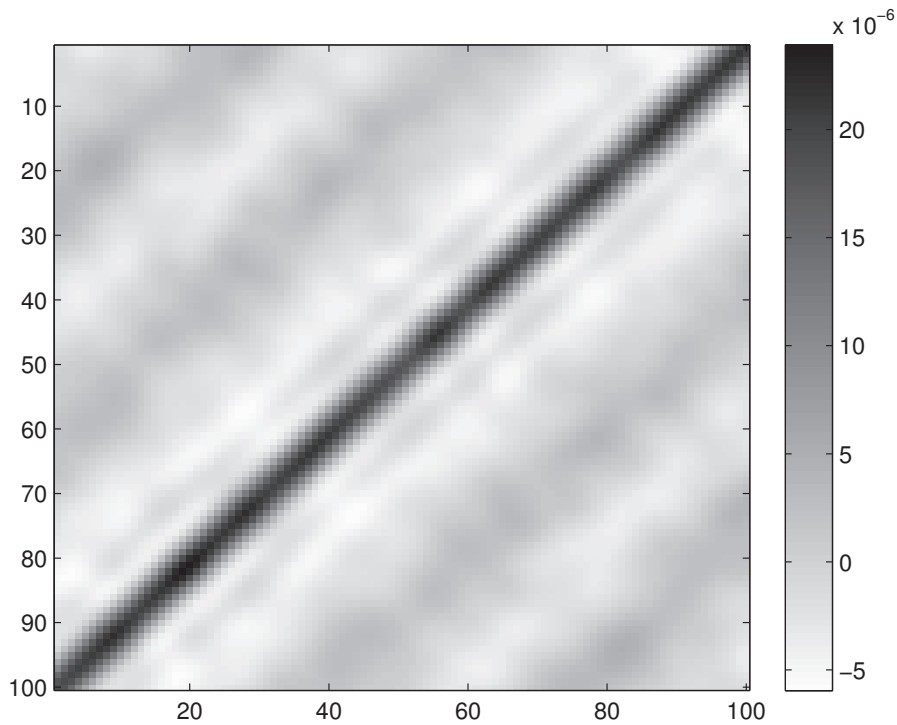


Fig. 4. Covariance matrix for the noise process (development set).

4.2.1 Noise whitening

If the additive noise is a colored noise, is desirable to apply a whitening filter (Whalen, 1995) on a preprocessing phase. When a given zero-mean signal \mathbf{y} is said white, its samples are uncorrelated and the corresponding variance is unitary (Hyvärinen, 2001). As a consequence, its covariance matrix equals de identity matrix:

$$E[\mathbf{y}\mathbf{y}^T] = \mathbf{I}. \tag{11}$$

It is possible to obtain a linear transformation that applied to a process \mathbf{y} produces a new signal process \mathbf{v} that is white. A common way to obtain the whitening transformation is through the decomposition of the covariance matrix into its eigenvalues and eigenvectors (Hyvärinen, 2001):

$$E[\mathbf{y}\mathbf{y}^T] = \mathbf{E}\mathbf{D}\mathbf{E}^T \tag{12}$$

where \mathbf{E} is the orthogonal matrix of eigenvectors and \mathbf{D} is the diagonal matrix of the eigenvalues. The whitening matrix is then obtained through (Hyvärinen, 2001):

$$\mathbf{W} = \mathbf{E}\mathbf{D}^{-1/2}\mathbf{E}^T. \tag{13}$$

And the signal transformation

$$\mathbf{v} = \mathbf{W}\mathbf{y} \tag{14}$$

obtains the white signal process \mathbf{v} .

The covariance matrix for the raw data (see Section 4.2.3 next) is shown in Fig. 4. The covariance matrix exhibits crosstalks, which point out a deviation from a fully white noise

process. The whitening transformation applied to the development set (see next section) results on a perfect diagonal matrix and the results are well generalized for the testing set (see Fig. 5).

4.2.2 Stochastic process detection

In this case, matched filter design may be generalized for stochastic process detection (Trees - Part III, 2001). For this more complex detection problem and assuming Gaussian process, the principal component analysis (PCA) (Jolliffe, 2010) is applied, and the meteor signal becomes decomposed into principal (deterministic) directions, which are obtained from the Karhunen-Loève series (Trees - Part I, 2001)

$$Y = \sum_{i=1}^N c_i \phi_i \quad (15)$$

The series coefficient c_i describes all the stochasticity of the process and ϕ_i is an eigenvector of the covariance matrix of the stochastic process (assumed to be zero-mean). Associated to each eigenvector, there is an eigenvalue λ_i , which represents the energy of the process retained in the direction of ϕ_i . The number of components to be extracted may be limited to a given amount of energy reconstruction, allowing signal compaction. The discarded components are typically associated to noise and do not help in the signal detection task. After decomposition, a filter is matched to each component, resulting in the detection system shown in Fig. 6.

In Fig. 6, h_i provides the weighting of each matched filter in the overall decision, corresponding to the energy fraction of each principal component (when the noise is with spectral height $N_0/2$):

$$h_i = \frac{\lambda_i}{N_0/2 + \lambda_i} \quad (16)$$

Typically, the masking noise process is not white and the detection system can be implemented as shown schematically in Fig.7.

Due to the fact that the detection must run online, the speed and complexity of the applied technique must be considered for the implementation. For meteor signals, the stochastic detection may roughly be approximated by considering the process represented by a deterministic target signal, which can be a specific event, considered the most representative of the process, or the process mean (see Fig. 8). This simplification has been successful in high-energy physics for particle detection (Ramos, 2004).

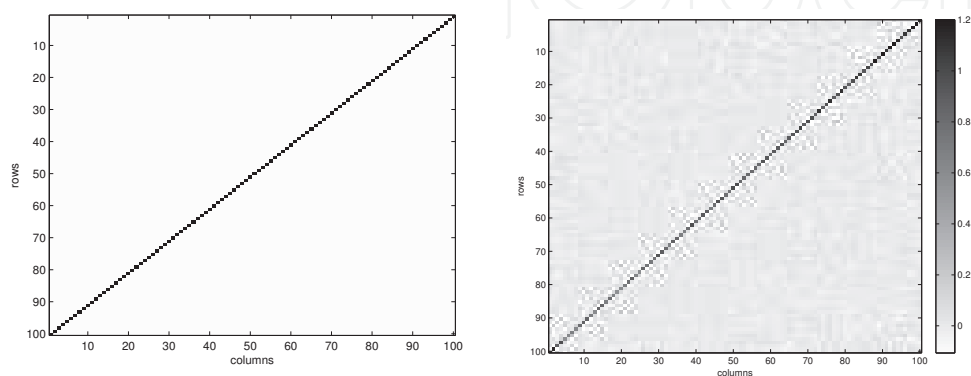


Fig. 5. Covariance matrix after whitening for both (a) development and (b) testing sets.

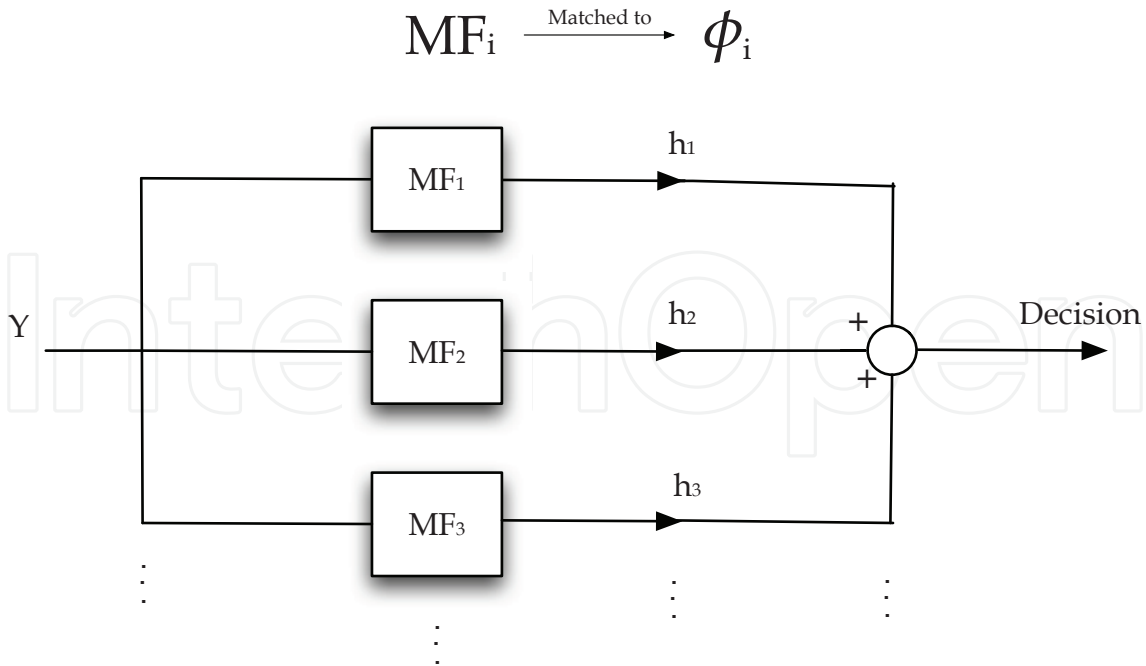


Fig. 6. Block diagram of the matched filter for stochastic signals.

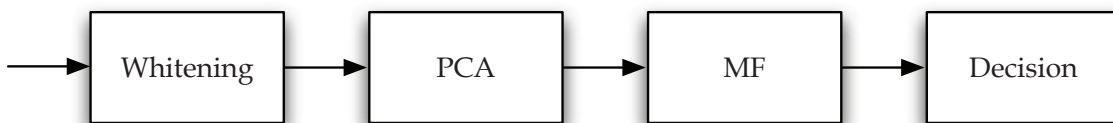


Fig. 7. Block diagram of the matched filter for stochastic signals considering colored noise.

4.2.3 Experimental data

Experimental meteor signals were selected through visual inspection and split into both development and test sets. The first set was used to design the filter, and the second to evaluate the generalization capability of the design and quotes the performance efficiency. Due to variations on signal width, a fixed time window of 1 second was chosen, which is large enough to accommodate most interesting events. Signals were synchronized by their peak values in the acquisition time windows. Noise data from different days of acquisition were also split into development and testing sets. Each noise data set comprised 500 signals, which were obtained through visual inspection. Fig. 9 shows a Gaussian fit applied to the noise histogram, which reveals that the noise may roughly be considered a zero-mean Gaussian process. This approximation facilitates the matched filter design, as shown above.

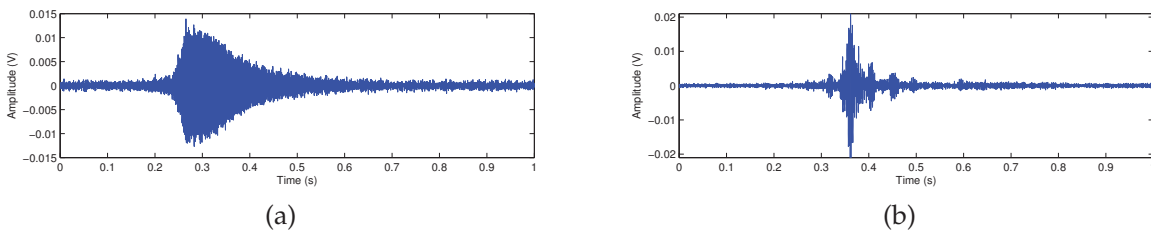


Fig. 8. Underdense trails signals: (a) typical event and (b) the process mean.

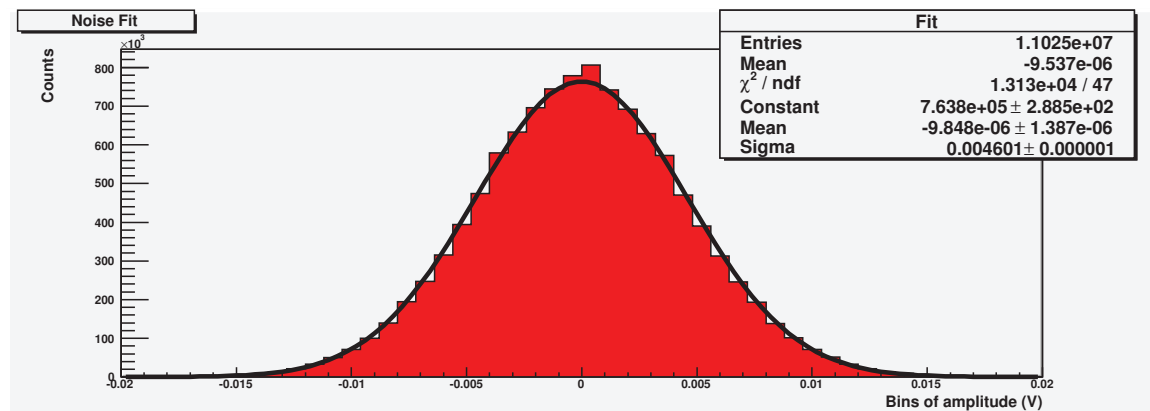


Fig. 9. Gaussian fit applied to noise histogram.

Some steps of the data acquisition, such as low-pass filtering, produced a colored noise, so that the whitening preprocessing should be applied in order to design the detection system based on a matched filter.

4.2.4 Filter performance

Considering the matched filter design approximation discussed in section 4.2.2, the best results for the detection based on matched filter were obtained using as a target signal the mean signal, which was obtained from underdense trails of the development set. Fig. 10 shows the ROC curves for the testing set for both the matched filter and simple threshold detection. It can be seen that the matched filter system achieves a much better performance. For the development set, the filter achieves an efficiency of 99.3% without committing errors of type-I. For an efficiency of 100%, the false alarm probability reaches 0.2%. For the test set, the numbers are 98.8% of detection efficiency for a P_F equal to zero and 1.5% of false alarm probability for 100% detection efficiency (see Fig. 10). Choosing the decision threshold by maximizing the SP index (see Fig. 11 (a)) leads us to an efficiency of 99.4%, for 0.2% of false alarm and considering the testing set.

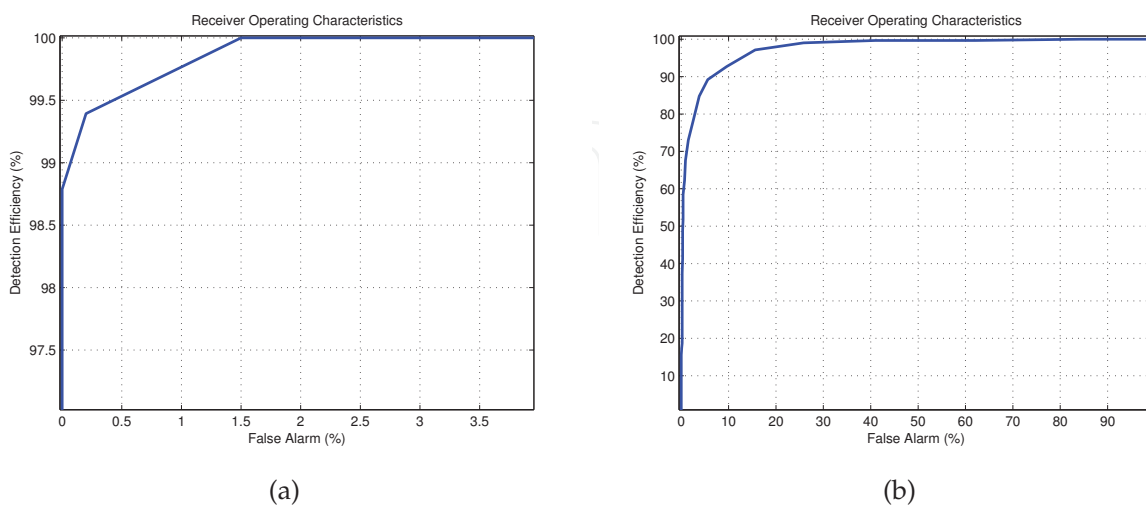


Fig. 10. ROC curves for: (a) matched filter (deterministic approach) and (b) for threshold detection. Both for testing set.

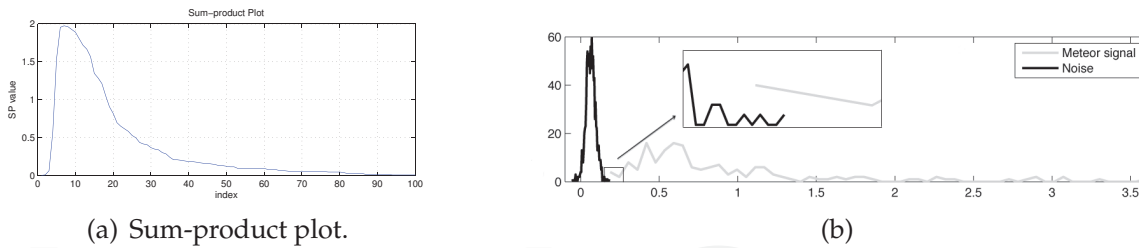


Fig. 11. (a) SP plot for choosing the decision threshold and (b) Filter output distributions (in the detail, the superposition of the curves for noise and meteor signal).

4.3 Frequency-domain analysis

Radar detection of meteors can also be performed in frequency-domain. The spectral information is obtained by applying the Fourier transform or its variants.

4.3.1 Cumulative spectral power analysis

In frequency-domain, the information about the meteor events is concentrated within a narrow band of the spectrum, corresponding to the demodulated video carrier. For a WSS random process, the power spectrum is defined as the Fourier transform of the autocorrelation sequence

$$S_y(\omega) = \sum_{k=-\infty}^{\infty} R_y(k)e^{-jk\omega}. \tag{17}$$

If only a segment of the signal of length N is available, the autocorrelation can be estimated through (Hayes, 1996)

$$\hat{R}_y(k) = \frac{1}{N} \sum_{n=0}^{N-1-k} y(n+k)y^*(n). \tag{18}$$

Changing the upper limit to $N - 1 - k$, we guarantee that only values of $y(n)$ in the range $[0, N - 1]$ will contribute to the sum. Now considering the signal $y_N(n)$, which results from the product of $y(n)$ with a rectangular window of length N samples,

$$y_N(n) = \begin{cases} y(n) & ; 0 \leq n < N - 1 \\ 0 & ; \text{otherwise} \end{cases}, \tag{19}$$

the estimate of the autocorrelation sequence becomes

$$\hat{R}_y(k) = \frac{1}{N} \sum_{n=-\infty}^{\infty} y_N(n+k)y_N^*(n). \tag{20}$$

Taking the Fourier transform and using the convolution theorem (Hayes, 1996),

$$\hat{S}_y(\omega) = \frac{1}{N} Y_N(\omega)Y_N^*(\omega) = \frac{1}{N} |Y_N(\omega)|^2 \tag{21}$$

where $Y_N(\omega)$ is the Fourier transform of $y_N(n)$. Thus, the power spectral density (PSD) is proportional to the squared magnitude of the Fourier transform. This estimate is known as periodogram (Hayes, 1996).

Blocks of 30s of acquired signal were windowed using non overlapping rectangular windows and the short-time Fourier transform (STFT) was applied (Oppenheim, 1989). Then, the PSD

is estimated via periodogram. Considering the sampling frequency of 22,050 Hz, windows of 256 samples correspond to a time length of approximately 11 ms, which provides a good resolution for the detection and allows wide-sense stationarity (Papoulis, 1965). The 30 s of acquired data were split into 2,584 windowed segments. For the data windows, the peak values are stored. Fig. 12 shows a spectrogram for a 30 s data block.

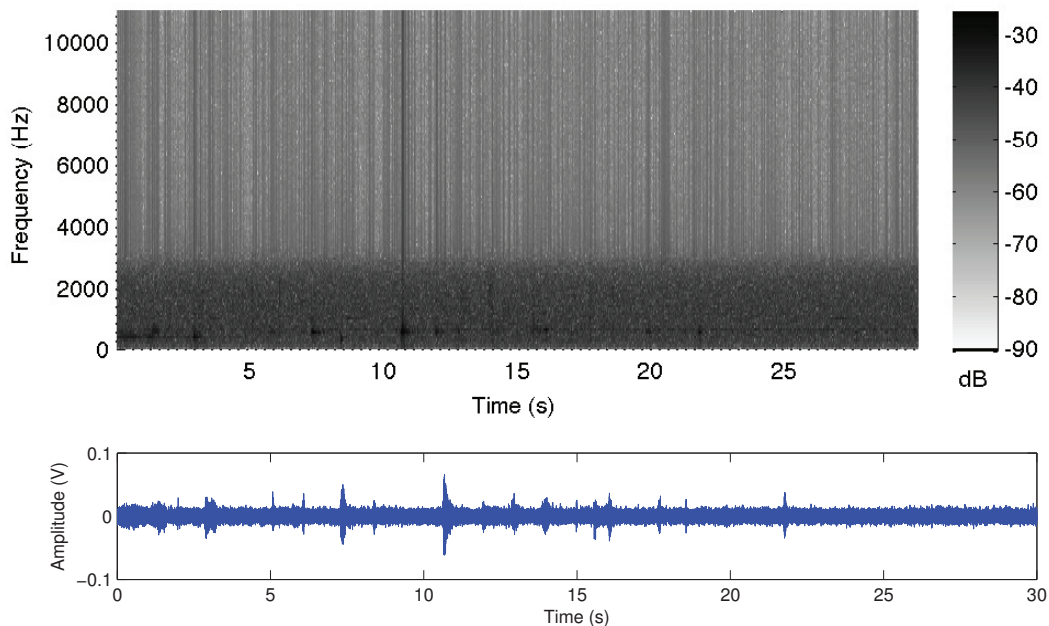


Fig. 12. Spectrogram for a 30s data block.

The obtained curve is then accumulated over all time windows, producing the curve shown in Fig.13. The accumulating process produces a curve that exhibits small fluctuation and monotonically increases. The slope in the cumulative power is due to the background noise and it is estimated through a straight-line fit (Fig. 13, dashed line), which is then subtracted from the curve. The resulting accumulated curve is also shown (thicker curve).

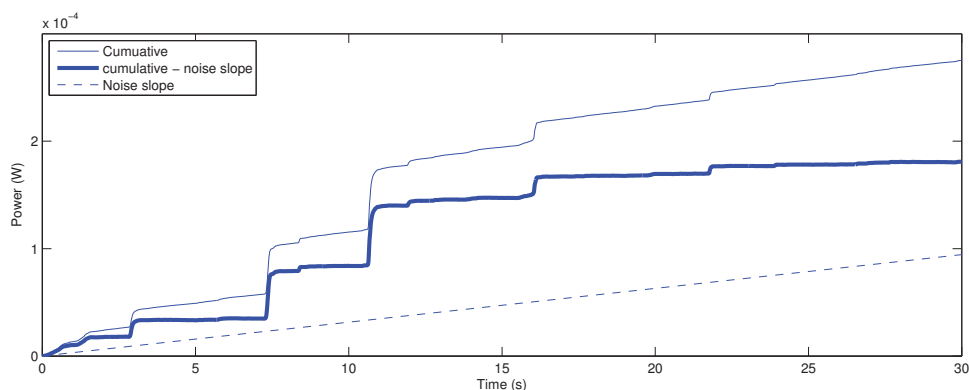


Fig. 13. Curves generated in the cumulative spectral power analysis.

Fluctuations in the slope threshold values are used to define the starting and ending samples for triggering. For the algorithm design, 40 blocks of acquired data were used, which comprised 233 meteor events. For evaluating the performance and generalization, 50 blocks comprising 261 meteor events were selected. Accumulating windows peak values, the cumulative power spectrum algorithm detected 17 fake events over 1,500 s of data (6.7 %

of false alarm), which means approximately 1 fake event per each 100 seconds. Therefore, from this test sample, the algorithm avoided 220 fake events to be recorded (280 MB less per hour). In a full day, the online filter would avoid 6.7 GB of noise to be recorded.

5. Summary and perspectives

Meteor signal detection has been addressed by different techniques. A new detection technique based on radar has advantages, as simplicity of the detection stations, coverage and capacity to be extended for other detection tasks, such as cosmic rays, lightning, among others. Due to its continuous acquisition characteristic, online triggering is mandatory for avoiding the storage of an enormous amount of background data and allow focusing on the interesting events in offline analysis. Both time and frequency domain techniques allow efficient meteor signal detection. The matched filter based system achieves the best performance, and has good advantages, such as it is easy to implement and has fast processing speed. In frequency domain, a power spectrum analysis also achieves good results. This approach may also be further developed to include a narrowband demodulation in the preprocessing phase. As phase delays are produced by the different paths the traveling wave finds between the transmission, oscillations can be observed (see Fig. 14) mainly in underdense trails. These reflections can be seen as an amplitude modulation, similar to the modulation on sonar noise caused by cavitation propellers (Moura et al., 2009).

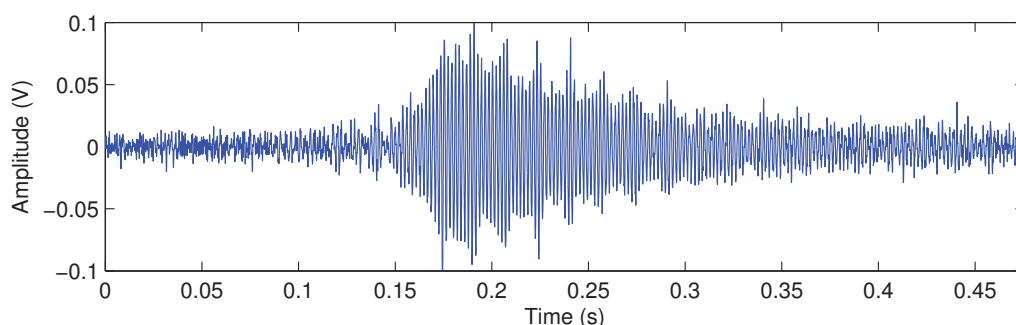


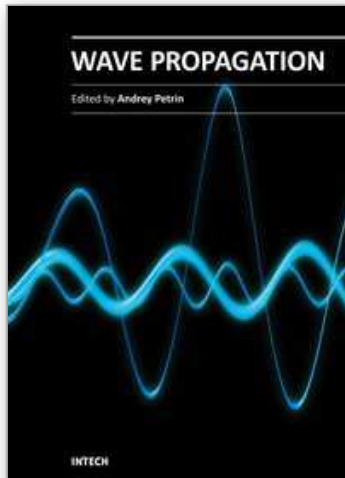
Fig. 14. Amplitude modulation on a underdense signal.

Therefore, a DEMON (Demodulation of Envelope Modulation On Noise) analysis may be applied. The acquired signal is filtered by a lowpass filter, to select the band of interest for the meteor signals. Then the signal is squared in a traditional amplitude demodulation, for the extraction of the envelope. Due to the low frequencies of the oscillations (typically tens of Hz), resampling is performed, after the anti-alias filtering. Finally a FFT is applied, and the frequency the envelope is identified. Other possible approach is to apply computational intelligence methods.

6. References

- Anjos, A. R. dos; Torres, R. C.; Seixas, J. M. de; Ferreira, B.C.; Xavier, T.C., *Neural Triggering System Operating on High Resolution Calorimetry Information*, Nuclear Instruments and Methods in Physics Research (A), v. 559, p. 134-138, 2006.
- Damazio, D. O., Takai, H., *The cosmic ray radio detector data acquisition system*, Nuclear Science Symposium Conference Record, 2004 IEEE, On page(s): 1205-1211 Vol. 2.
- Fawcett, T. *An introduction to ROC analysis*. Pattern Recognition Letters, 27, 861-874, 2006.

- Guang-jie, W., Zhou-sheng, Z. *Video observation of meteors at Yunnan Observatory*. Chinese Astronomy and Astrophysics, Volume 28, Issue 4, October-December 2004, Pages 422-431.
- Hayes, M.H. *Statistical Digital Signal Processing and Modeling*, ISBN: 0-471-59431-8, John Wiley and Sons Inc., New York, 1996.
- Hirose H., Tomita, K., *Photographic Observation of Meteors*. Proceedings of the Japan Academy, Vol.26, No.6(1950)pp.23-28.
- Hyvärinen, A., Karhunen, J. and Oja, E. (2001). *Independent Component Analysis*, ISBN: 0-471-40540-X, John Wiley & Sons, .inc. 2001.
- International Meteor Organization, www.imo.net, access September, 2010.
- Jolliffe, I.T., *Principal Components Analysis*, ISBN: 0-387-95442-2, second edition, Springer New York, 2010.
- McKinley, D.W.R., *Meteor Science and Engineering*, Ed. McGraw-Hill Book Company, New York 1961.
- Matano, M. Nagano, K. Suga and G. Tanahashi. Can J. Phys. 46 (1968), p. S255.
- Moura, M. M., Filho, E. S., Seixas, J .M., 'Independent Component Analysis for Passive Sonar Signal Processing', chapter 5 in *Advances in Sonar Technology*, ISBN:978-3-902613-48-6, In-Teh, 2009.
- Oppenheim, A.V., and R.W. Schaffer, *Discrete-Time Signal Processing*, Prentice-Hall, 1989, pp.730-742.
- Papoulis, A., *Probability, Random Variables, and Stochastic Processes*, ISBN: 0-07-048448-1, McGraw-Hill Book Company Inc., New York, 1965.
- Ramos, R. R., Seixas, J. M., *A Matched Filter System for Muon Detection with Tilecal*. Nuclear Instruments & Methods in Physics Research, v. 534, n. 1-2, p. 165-169. 2004.
- Shamugan, K.S., Breipohl, A.M. *Random Signals - detection, estimation and data analysis*, John Wiley & Sons, New York, 1998.
- Trees, H.L.Van. *Detection, Estimation, and Modulation Theory, Part I*, ISBN: 0-471-09517-6, John Wiley & Sons, New York, 2001.
- Trees, H.L.Van. *Detection, Estimation, and Modulation Theory, Part III*, ISBN: 0-471-10793-X, John Wiley & Sons, New York, 2001.
- Whalen A. D. *Detection of Signals in Noise*. Second Edition. ISBN: 978-0127448527, Academic Press, 1995.
- Willis, N.C., 'Bistatic Radar', chapter 23 in *Radar Handbook*, third edition, (M.I. Skolnik ed.), ISBN 978-0-07-148547-0, McGraw-Hill, New York, 2008.
- Wislez, J. M. *Forward scattering of radio waves of meteor trails*, Proceedings of the International Meteor Conference, 83-98, September 1995.



Wave Propagation

Edited by Dr. Andrey Petrin

ISBN 978-953-307-275-3

Hard cover, 570 pages

Publisher InTech

Published online 16, March, 2011

Published in print edition March, 2011

The book collects original and innovative research studies of the experienced and actively working scientists in the field of wave propagation which produced new methods in this area of research and obtained new and important results. Every chapter of this book is the result of the authors achieved in the particular field of research. The themes of the studies vary from investigation on modern applications such as metamaterials, photonic crystals and nanofocusing of light to the traditional engineering applications of electrodynamics such as antennas, waveguides and radar investigations.

How to reference

In order to correctly reference this scholarly work, feel free to copy and paste the following:

Eric V. C. Leite, Gustavo de O. e Alves, José M. de Seixas, Fernando Marroquim, Cristina S. Vianna and Helio Takai (2011). Radar Meteor Detection: Concept, Data Acquisition and Online Triggering, Wave Propagation, Dr. Andrey Petrin (Ed.), ISBN: 978-953-307-275-3, InTech, Available from:

<http://www.intechopen.com/books/wave-propagation/radar-meteor-detection-concept-data-acquisition-and-online-triggering>

INTECH
open science | open minds

InTech Europe

University Campus STeP Ri
Slavka Krautzeka 83/A
51000 Rijeka, Croatia
Phone: +385 (51) 770 447
Fax: +385 (51) 686 166
www.intechopen.com

InTech China

Unit 405, Office Block, Hotel Equatorial Shanghai
No.65, Yan An Road (West), Shanghai, 200040, China
中国上海市延安西路65号上海国际贵都大饭店办公楼405单元
Phone: +86-21-62489820
Fax: +86-21-62489821

© 2011 The Author(s). Licensee IntechOpen. This chapter is distributed under the terms of the [Creative Commons Attribution-NonCommercial-ShareAlike-3.0 License](#), which permits use, distribution and reproduction for non-commercial purposes, provided the original is properly cited and derivative works building on this content are distributed under the same license.

IntechOpen

IntechOpen